
Memory Efficient Meta-Learning with Large Images

John Bronskill*
University of Cambridge
jfb54@cam.ac.uk

Daniela Massiceti*
Microsoft Research
dmassiceti@microsoft.com

Massimiliano Patacchiola*
University of Cambridge
mp2008@cam.ac.uk

Katja Hofmann
Microsoft Research
kahofman@microsoft.com

Sebastian Nowozin
Microsoft Research
senowoz@microsoft.com

Richard E. Turner
University of Cambridge
ret26@cam.ac.uk

Abstract

Meta learning approaches to few-shot classification are computationally efficient at test time, requiring just a few optimization steps or single forward pass to learn a new task, but they remain highly memory-intensive to train. This limitation arises because a task’s entire support set, which can contain up to 1000 images, must be processed before an optimization step can be taken. Harnessing the performance gains offered by large images thus requires either parallelizing the meta-learner across multiple GPUs, which may not be available, or trade-offs between task and image size when memory constraints apply. We improve on both options by proposing LITE, a general and memory efficient episodic training scheme that enables meta-training on large tasks composed of large images on a single GPU. We achieve this by observing that the gradients for a task can be decomposed into a sum of gradients over the task’s training images. This enables us to perform a forward pass on a task’s entire training set but realize significant memory savings by back-propagating only a random subset of these images which we show is an unbiased approximation of the full gradient. We use LITE to train meta-learners and demonstrate new state-of-the-art accuracy on the real-world ORBIT benchmark and 3 of the 4 parts of the challenging VTAB+MD benchmark relative to leading meta-learners. LITE also enables meta-learners to be competitive with transfer learning approaches but at a fraction of the test time computational cost, thus serving as a counterpoint to the recent narrative that transfer learning is all you need for few-shot classification.

1 Introduction

Meta-learning approaches to few-shot classification are very computationally efficient. Once meta-trained, they can learn a new task at test time with as few as 1-5 optimization steps [1, 2] or a single forward pass through the model [3–5] and with minimal or no hyper-parameter tuning. In contrast, transfer learning approaches based on fine-tuning typically rely on a large pre-trained feature extractor, and instead take 100s-1000s of optimization steps at test time in order to learn a task [6], thus incurring a high computational cost for each new task encountered. This makes meta-learned solutions attractive in compute-constrained deployments, or scenarios where the model must learn multiple different tasks or update on-the-fly (e.g. in continual and online learning settings [7–10]).

However, a crucial barrier to progress is that meta-learning approaches are memory-intensive to train and thus cannot easily leverage large images for a performance boost, as recent fine-tuning approaches have done. This limitation arises because a meta-learner must back-propagate through *all*

*Authors contributed equally

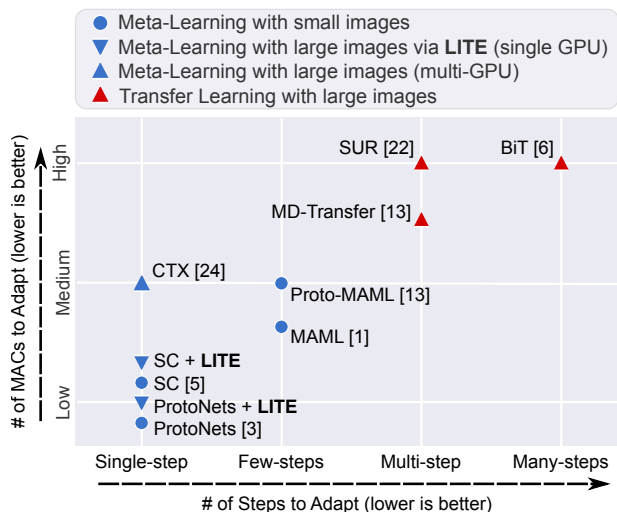


Figure 1: **LITE enables meta-learners to be trained on large images with one GPU thereby significantly improving performance while retaining their test time computational efficiency.** The schematic shows test time efficiency (the number of steps and number of Multiply-Accumulate operations (MACs) needed to learn a new task at test time) and whether the method can be trained on large images (required for good performance). Existing meta-learners are cheap to adapt but trained on small images (multiple GPUs are required for large images), transfer learning methods are expensive to adapt but trainable on large images. Meta-learners with LITE get the best of both worlds. Note: SC + LITE is Simple CNAPs [5] trained with LITE.

the examples in a task’s support set (i.e. the task’s training set) that contribute to a prediction on a query example. In some cases, this can be as many as 1000 images [11]. As a result, the amount of memory required for the computational graph grows linearly with the number of support images, and quadratically with their dimension. In contrast, transfer learning approaches can employ standard batch processing techniques to scale to larger images when under memory constraints — a feature which has contributed significantly to their recent success on few-shot benchmarks [11].

Current solutions for training meta-learners on large images include 1) parallelizing the model across multiple GPUs, which may not be available or convenient, 2) considering tasks with fewer support images, and 3) employing gradient/activation checkpointing methods [12] which incur longer training times and still fall short of the task sizes required in key benchmarks. Instead, most existing work [1, 3, 2, 13, 4, 14] has opted for training on large tasks but small images which translates poorly into real-world applications and limits competitiveness on few-shot benchmarks.

In this work, we improve on these alternatives by proposing LITE, a Large Image *and* Task Episodic training scheme for meta-learning models that enables training with large images and large tasks, on a single GPU. We achieve this through the simple observation that meta-learners typically aggregate a task’s support examples using a permutation invariant sum operation. This structure ensures invariance to the ordering of the support set. Consequently, the gradients for a task can be decomposed as a sum of gradient contributions from the task’s support examples. This enables us to perform a forward pass on a task’s entire support set, but realize significant savings in memory by back-propagating only a random subset of these images which we show is an unbiased approximation of the true gradient. Fig. 1 illustrates the key trade-offs, with LITE enabling meta-learners to benefit from large images for improved classification accuracy but still remain computationally efficient at test time.

We use LITE to train key meta-learning methods and show that our best performing instantiation – Simple CNAPs [5] with LITE – achieves state-of-the-art results relative to all meta-learners on two challenging few-shot benchmarks: VTAB+MD [11], an extensive suite of both meta-learning and transfer learning tasks, and ORBIT [14], an object recognition benchmark of high-variation real-world videos. Our results showcase the unique advantage of meta-learning methods – that when properly trained they can be competitive with transfer learning approaches in terms of accuracy for a fraction of the computational cost at test time — and they serve as a counterpoint to the recent narrative that transfer learning is all you need for few-shot classification.

Our contributions

1. LITE, a general and memory-efficient episodic training scheme which enables meta-learning models to be trained on large images and large tasks on a single GPU.
2. A mathematical justification for approximating the true gradient with a random subset of a task’s support examples which applies to common classes of meta-learning methods.
3. Instantiations of LITE on key classes of meta-learners to demonstrate its versatility.

4. State-of-the-art performance using Simple CNAPs with LITE compared to other leading meta-learners on two challenging few-shot benchmarks, VTAB+MD and ORBIT ²

2 Why Meta-Learning with Large Images and Tasks is Difficult

Meta-learning preliminaries In few-shot image classification, the goal is to recognize new classes when given only a few training (or support) images of each class. Meta-learners typically achieve this through *episodic* training [15]. Here, an episode or task τ contains a support set $\mathcal{D}_S^\tau = \{(\mathbf{x}_n^\tau, y_n^\tau)\}_{n=1}^{N_\tau}$ and a query set $\mathcal{D}_Q^\tau = \{(\mathbf{x}_m^{\tau*}, y_m^{\tau*})\}_{m=1}^{M_\tau}$, where (\mathbf{x}, y) is an image-label pair, N_τ is the number of (labeled) support elements given to learn the new classes, and M_τ is the number of query elements requiring predictions. Note that in a given task, elements in \mathcal{D}_Q^τ are drawn from the same set of classes as the elements in \mathcal{D}_S^τ . For brevity we may use the shorthand $\mathcal{D}_S = \{\mathbf{x}, y\}$ and $\mathcal{D}_Q = \{\mathbf{x}^*, y^*\}$.

During meta-training, a meta-learner is exposed to a large number of training tasks $\{\tau\}$. For each task τ , the meta-learner takes as input the support set \mathcal{D}_S and outputs the parameters of a classifier that has been adapted to the current task $\theta^\tau = \theta_\phi(\mathcal{D}_S)$. The classifier can now make task-specific probabilistic predictions $f(\mathbf{x}^*, \theta^\tau = \theta_\phi(\mathcal{D}_S))$ for any query input \mathbf{x}^* (see Fig. 2). A function $\mathcal{L}(y^*, f(\mathbf{x}^*, \theta^\tau))$ computes the loss between the adapted classifier’s predictions for the query input and the true label y^* which is observed during meta-training. Assuming that \mathcal{L} , f , and $\theta_\phi(\mathcal{D}_S)$ are differentiable, the meta-learner can then be trained with stochastic gradient descent by back-propagating the loss and updating the parameters ϕ .

At meta-test time, the trained meta-learner is given a set of unseen test tasks, which typically contain classes that have *not* been seen during meta-training. For each task, the meta-learner is given its support set \mathcal{D}_S , and is then evaluated on its predictions for all the query inputs \mathbf{x}^* (Fig. 2, left).

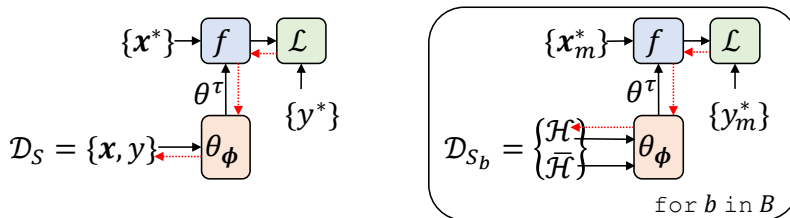


Figure 2: Left: Canonical meta-learner. Right: Meta-learner with LITE. The red dotted line shows the back-propagated gradients. Refer to Algorithm 1 for nomenclature.

Large memory requirements for meta-training The primary bottleneck to using large images (i.e. $\geq 224 \times 224$ pixels) in meta-learning approaches is the large amount of (GPU) memory required to process a task’s support set \mathcal{D}_S during meta-training. Specifically, the meta-learner $\theta_\phi(\mathcal{D}_S)$ must perform a forward pass with a task’s *entire* support set before it can back-propagate the loss for query elements $(\mathbf{x}^*, y) \in \mathcal{D}_Q$ (and release the computation graph), thus preventing the use of conventional batch processing. The amount of memory required scales linearly with the number of support images N^τ and quadratically with their dimensions. If N^τ is large (e.g. the recent VTAB+MD benchmark [11] requires a task’s support set to be as large as 1000 images), memory on a single GPU is thus quickly exceeded for large images.

Note, the number of query elements in the task M^τ is not a bottleneck when using large images as the loss decomposes over elements of the query set \mathcal{D}_Q and is therefore amenable to mini-batching. By contrast, as the classifier itself is a non-linear function of the *support set*, the loss does not decompose and so it is not obvious how to apply similar ideas to allow scaling of \mathcal{D}_S in a principled way.

Current ad hoc solutions to this problem are: (i) parallelize the meta-learner across multiple GPUs which may not be convenient or available and can involve significant engineering effort; (ii) train on tasks with smaller (or sub-sampled) support sets which may adversely affect performance on test tasks with more classes and/or large numbers of samples per class; (iii) train on tasks with smaller images (e.g. 84×84 pixels in *miniImageNet* [16]) which limits performance and translates poorly to many real-world applications; or (iv) trade memory usage for additional computation [12] by

²Source code for ORBIT experiments is available at <https://github.com/microsoft/ORBIT-Dataset> and for the VTAB+MD experiments at <https://github.com/cambridge-mlg/LITE>.

Algorithm 1 LITE for a meta-training task τ

Require: \mathcal{D}_S : task support set; \mathcal{D}_Q : task query set; N : number of support examples in \mathcal{D}_S ; H : number of elements in \mathcal{D}_S to back-propagate; M : number of query examples in \mathcal{D}_Q ; M_b : batch size for \mathcal{D}_Q ; $\text{backward}() \equiv$ function to back-propagate a loss; $\text{step}() \equiv$ function to update parameters with a gradient step.

```
1:  $B \leftarrow \text{ceil}(M/M_b)$  ▷ number of query batches
2: for all  $b \in 1, \dots, B$  do
3:    $\mathcal{D}_{Q_b} \leftarrow \{\mathbf{x}_m^*, y_m^*\}_{m=1}^{M_b}$  ▷ get query batch from  $\mathcal{D}_Q$ 
4:    $\mathcal{H} \leftarrow \{(\mathbf{x}_{n_h}, y_{n_h})\}_{h=1}^H$  where  $\{n_h\}_{h=1}^H \sim \mathcal{U}(1, N)$  ▷  $\mathcal{H}$  to back-propagate
5:    $\overline{\mathcal{H}} \leftarrow \mathcal{D}_S \cap \overline{\mathcal{H}}$  ▷  $\overline{\mathcal{H}}$  to not back-propagate
6:    $\mathcal{D}_{S_b} \leftarrow \mathcal{H} \cup \overline{\mathcal{H}}$ 
7:    $\boldsymbol{\theta}^\tau \leftarrow \boldsymbol{\theta}(\mathcal{D}_{S_b})$ 
8:    $L_b \leftarrow \frac{1}{M_b} \sum_{m=1}^{M_b} \mathcal{L}(y_m^*, f(\mathbf{x}_m^*, \boldsymbol{\theta}^\tau))$  ▷ get loss of query batch
9:    $\text{backward}(L_b)$  ▷ back-propagate loss on query batch
10: end for
11:  $\phi \leftarrow \text{step}(\phi, N/H)$  ▷ update  $\phi$  using weighting factor  $N/H$ 
```

employing *activation/gradient checkpointing* (i.e. during training store only a subset of intermediate activations in a network needed for backpropagation and recompute the rest with additional forward computations when needed) which allows for training on larger tasks at the expense of training time, but still falls well short of the memory needed to accommodate the task sizes required for key benchmarks (e.g. VTAB+MD).

Although training meta-learners has large memory requirements, meta-testing is generally memory efficient, requiring only a small number of gradient operations, or none at all, compared to transfer learning approaches that would perform large numbers of gradient-based updates at test time.

3 Large Image and Task Episodic (LITE) training

In this section, we introduce our general and memory-efficient solution for training meta-learners episodically on tasks with large support sets and large images. We call our approach *Large Image and Task Episodic* training or LITE. In Section 3.1, we describe how LITE can be applied to key classes of meta-learners.

Approach The fundamental idea underlying LITE is to perform a forward pass using the entire support set \mathcal{D}_S , but to compute the gradient contribution on only a small random subset of the examples in the support set. By doing this, we realize large savings in memory that includes gradients, activations, and the computation graph for the elements of \mathcal{D}_S that are not back-propagated. This is an approximation of the true gradient that would result if back-propagation was performed on all of the examples in \mathcal{D}_S . In the following section, we show that this approximation is an unbiased estimate of the true gradient. The approach for a general meta-learner is detailed in Algorithm 1 and shown diagrammatically in Fig. 2.

Mathematical justification The parameters of the meta-learner ϕ are found by minimizing the expected loss over all tasks.

$$\underset{\phi}{\operatorname{argmin}} \sum_{\tau=1}^T \sum_{m=1}^{M_\tau} \mathcal{L}(y_m^{\tau*}, f(\mathbf{x}_m^{\tau*}, \boldsymbol{\theta}_\phi(\mathcal{D}_S^\tau))). \quad (1)$$

In most meta-learning approaches, the support set enters into the loss through a sum over the N individual contributions from each data point it contains. This structure enables the meta-learners to be invariant to the ordering of the support set and allows all members of the support set to contribute to the adapted parameters (unlike alternative permutation invariant operators like *max* or *min*). Below we show in blue how this sum arises in popular brands of meta-learners.

In amortization methods (e.g. CNAPS [4] and VERSA [17]), the aggregation of support set points is built in directly via a deep set encoder $e_{\phi_1}(\cdot)$. This encodes the support set into an embedding vector

which is mapped to the classifier parameters by a hyper-network $t_{\phi_0}(\cdot)$.

$$\boldsymbol{\theta}_\phi(\mathcal{D}_S) = t_{\phi_0} \left(\sum_{n=1}^N e_{\phi_1}(\mathbf{x}_n, y_n) \right). \quad (2)$$

In gradient-based methods (e.g. MAML [1]), the classifier parameters are adapted from an initial value ϕ_0 using a sum of derivatives of an inner-loop loss computed for each data point in the support set. The derivatives play the role of the deep set encoder in amortization methods.

$$\boldsymbol{\theta}_\phi(\mathcal{D}_S) = \phi_0 + \phi_1 \sum_{n=1}^N \frac{d}{d\phi} \mathcal{L}_{\text{inner}}(y_n, f(\mathbf{x}_n, \phi)) \Big|_{\phi=\phi_0} \quad (3)$$

Metric-based methods (e.g. ProtoNets [3]) comprise a body formed of a feature extractor and a head formed from a distance-based classifier. The classifier’s body parameters are not adapted in a task specific way $\boldsymbol{\theta}_{\phi,c}^{(\text{body})}(\mathcal{D}_S) = \phi_0$. The classifier’s head is adapted by averaging the activations for each class in the support set to form prototypes. Letting k_c denote the number of support examples of class c , the adapted head parameters are given by

$$\boldsymbol{\theta}_{\phi,c}^{(\text{head})}(\mathcal{D}_S) = \frac{1}{k_c} \sum_{i=1}^{k_c} f(\mathbf{x}_i^{(c)}, \phi_0) = \frac{1}{k_c} \sum_{n=1}^N \mathbb{1}(y_n = c) f(\mathbf{x}_n, \phi_0). \quad (4)$$

Query points can then be classified using their distance from these prototypes $d(f(\mathbf{x}_n^*, \phi_0), \boldsymbol{\theta}_{\phi,c}^{(\text{head})})$.

We have established that in many meta-learners, each support set affects the classifier parameters and therefore the loss through a sum of contributions from each of its elements. We now focus on the consequences of this structure on the gradients of the loss with respect to the meta-learner’s parameters. To reduce clutter, we consider the contribution from just a single query point from a single task and suppress the dependence of the loss on the classifier and the query data point, writing

$$\mathcal{L}(y^*, f(\mathbf{x}^*, \boldsymbol{\theta}_\phi(\mathcal{D}_S))) = \mathcal{L}(e_\phi(\mathcal{D}_S)) \quad \text{where} \quad e_\phi(\mathcal{D}_S) = \sum_{n=1}^N e_\phi(\mathbf{x}_n, y_n) = \sum_{n=1}^N e_\phi^{(n)}. \quad (5)$$

As a consequence of the summation, the derivative of the loss is given by

$$\frac{d}{d\phi} \mathcal{L}(e_\phi(\mathcal{D}_S)) = \mathcal{L}'(e_\phi(\mathcal{D}_S)) \times \left(\sum_{n=1}^N \frac{de_\phi^{(n)}}{d\phi} \right) \quad \text{where} \quad \mathcal{L}'(e_\phi(\mathcal{D}_S)) = \frac{d\mathcal{L}(e)}{de} \Big|_{e=e_\phi(\mathcal{D}_S)} \quad (6)$$

which is a product of the sensitivity of the loss to the encoding of the data points and the sensitivity of the contribution to the encoding from each data point w.r.t. the meta-learner’s parameters. This second term is the source of the memory overhead when training meta-learners, but importantly, it can be rewritten as an expectation w.r.t. a uniform distribution over the support set data-point indices,

$$\frac{d}{d\phi} \mathcal{L}(e_\phi(\mathcal{D}_S)) = N \mathcal{L}'(e_\phi(\mathcal{D}_S)) \mathbb{E}_{n \sim \mathcal{U}(1,N)} \left[\frac{de_\phi^{(n)}}{d\phi} \right]. \quad (7)$$

We can now define the LITE estimator of the loss-derivative by approximating the expectation by Monte Carlo sampling H times,

$$\frac{d}{d\phi} \mathcal{L}(e_\phi(\mathcal{D}_S)) \approx \frac{N}{H} \mathcal{L}'(e_\phi(\mathcal{D}_S)) \sum_{h=1}^H \frac{de_\phi^{(n_h)}}{d\phi} = \frac{d}{d\phi} \hat{\mathcal{L}}(e_\phi(\mathcal{D}_S)) \quad \text{where} \quad \{n_h\}_{h=1}^H \sim \mathcal{U}(1,N). \quad (8)$$

This estimator is unbiased, converging to the true gradient as $H \rightarrow \infty$. The estimator does not simply involve subsampling of the support set – parts of it depend on all the support set data points \mathcal{D}_S – and this is essential for it to be unbiased. The expectation and variance of this estimator are

$$\mathbb{E}_{\{n_h\} \sim \mathcal{U}(1,N)} \left[\frac{d\hat{\mathcal{L}}}{d\phi} \right] = \frac{d\mathcal{L}}{d\phi} \quad \text{and} \quad \mathbb{V}_{\{n_h\} \sim \mathcal{U}(1,N)} \left[\frac{d\hat{\mathcal{L}}}{d\phi} \right] = \frac{N^2}{H} (\mathcal{L}')^2 \mathbb{V}_{\{n_h\} \sim \mathcal{U}(1,N)} \left[\frac{de_\phi^{(n_h)}}{d\phi} \right].$$

In Section 5.3, we empirically show that the LITE gradient estimate is unbiased and that its standard deviation is smaller than that of the naive estimator formed by sub-sampling the full support set. LITE provides memory savings by subsampling H examples from the support set, with $H < N$, and back-propagating only them. Crucially, a forward pass is still performed with the complementary set of points, with cardinality $N - H$, but these are not back-propagated.

3.1 Applying LITE to key meta-learning approaches

To demonstrate its versatility, we now describe how to apply LITE to models within some of the main classes of meta-learners: CNAPs [4] and Simple CNAPs [5] for amortization-based methods and ProtoNets [3] for metric-based methods. Note, these are a few possible instantiations. LITE can be applied to other meta-learning methods in a straightforward manner.

In the descriptions below, we consider just one query batch \mathcal{D}_{Q_b} (i.e. one iteration of the for-loop in Algorithm 1). Note, in practice, whenever \mathcal{H} is passed through a module, back-propagation is enabled, while for $\overline{\mathcal{H}}$, back-propagation is disabled.³ Furthermore, since typically $|\mathcal{H}| \ll |\overline{\mathcal{H}}|$, we can forward \mathcal{H} in a single batch, however, we need to split $\overline{\mathcal{H}}$ into smaller batches. Since $\overline{\mathcal{H}}$ does not require gradients to be computed, this can be done without a significant impact on memory.

CNAPs [4], Simple CNAPs [5] + LITE (Appendix A.1) CNAPs variants are amortization-based methods whose hyper-networks take a task’s support set as input and generate FiLM layer [18] parameters which modulate a fixed feature extractor. The classifier head can also be generated (CNAPs [4]) or adopt a metric-based approach (Simple CNAPs [5]), thus both variants can be adapted with just a single forward pass of the support set at test time. Meta-training them with LITE involves passing \mathcal{H} and then $\overline{\mathcal{H}}$ through their set-encoder e_{ϕ_1} , and then averaging all the low-dimensional embeddings to get an embedding for the task. The task embedding is then input into a set of MLPs which generate FiLM layer parameters. \mathcal{H} is passed through this configured feature extractor, followed by $\overline{\mathcal{H}}$, to get the task-adapted features for all support examples in \mathcal{D}_{S_b} . For CNAPs, the task-adapted features of \mathcal{H} and $\overline{\mathcal{H}}$ are pooled by class and fed into a second MLP which generates the parameters of the fully-connected classification layer. For Simple CNAPs, the task-adapted features of \mathcal{H} and $\overline{\mathcal{H}}$ are instead used to compute class-wise distributions (i.e. class mean and covariance matrices). With back-propagation enabled, the query batch \mathcal{D}_{Q_b} is then passed through the task-configured feature extractor and classified with the task-configured classifier (for CNAPs), or with the Mahalanobis distance [19] to the class-wise distributions (for Simple CNAPs). The query batch loss is computed, and only back-propagated for \mathcal{H} . Note that the feature extractor is pre-trained and frozen, and only the parameters of the set-encoder and generator MLPs are learned.

ProtoNets [3] + LITE (Appendix A.2) ProtoNets [3] is a metric-based approach which computes a set of class prototypes from the support set and then classifies query examples by their (e.g. Euclidean) distance to these prototypes. Like CNAPs variants, it requires only a single forward pass to learn a new task. Meta-training ProtoNets with LITE involves passing \mathcal{H} through the feature extractor with back-propagation enabled, followed by $\overline{\mathcal{H}}$ with back-propagation disabled, to obtain features for all support examples \mathcal{D}_{S_b} . These features are averaged by class to compute the prototypes such that (with back-propagation enabled) the query batch \mathcal{D}_{S_b} can be passed through the feature extractor and classified based on the Euclidean distance. The loss of the query batch is computed and only back-propagated for \mathcal{H} . Note that here all the parameters of the feature extractor are learned.

4 Related work

We review the two main approaches to few-shot learning: transfer learning methods which are easy to scale to large images but are costly to adapt at test time, and meta-learning methods which are harder to scale but cheap to adapt (see Fig. 1). Note, we do not cover methods already described above.

Transfer learning approaches have demonstrated state-of-the-art performance on challenging few-shot benchmarks [20, 11]. However, they incur a high computational cost at test time as they rely on large (pre-trained) feature extractors which are fine-tuned with many optimization steps. MD-Transfer [13] fine-tunes all the parameters in a ResNet18 feature extractor with a cosine classifier head for 200 optimization steps. BiT [6] fine-tunes a feature extractor (pre-trained on 300M images in the JFT-300M dataset [21]) with a linear head, in some cases for up to 20,000 optimization steps to achieve its state-of-the-art results on the VTAB [20] benchmark. SUR [22] instead trains 7 ResNet-50 feature extractors, one for each training dataset. At test time, the predictions from each are concatenated and fine-tuned to minimize a cosine-similarity loss. All of these approaches involve on the order of teras to petas of Multiply-Accumulate operations (MACs) to learn a single new test task, and this must

³In PyTorch, this can be achieved by setting `torch.grad.enabled = True` when passing \mathcal{H} , and `torch.grad.enabled = False` when passing $\overline{\mathcal{H}}$.

be repeated for each new task encountered. Furthermore, for each new task type, transfer learning approaches may need to be tuned on a validation set to obtain the optimal hyper-parameters.

In comparison, meta-learning approaches [23] generally require orders of magnitude fewer MACs and steps to learn a new task at test time. Popular approaches include CNAPs [4], Simple CNAPs [5], ProtoNets [3], and MAML [1] and are discussed in Section 3.1. Others include ProtoMAML [13] which fuses ProtoNets and MAML by initializing the classifier weights with the prototypes and then, like MAML, takes a few optimization steps to tune the weights to the task. It therefore incurs a similar cost to adapt as MAML, except it must additionally compute the prototypes. Finally, CTX [24] replaces the final average pooling layer of ProtoNets with a transformer layer that generates a series of prototypes which are spatially aware and aligned with the task. Like CNAPs, it requires just a single forward pass, however, requires more MACs to adapt since it uses a larger feature extractor (ResNet-34) and an attention module. CTX is one of the few meta-learning approaches that has been meta-trained on 224×224 images, but requires 7 days of training on 8 GPUs.

Memory efficient variants of MAML have been developed. First-order MAML [1] saves memory by avoiding the estimate of second-order derivatives. This is also done in Reptile [25] that additionally avoids unrolling the computation graph, performing standard gradient descent at each adaptation step. Implicit MAML [26], decouples the meta-gradient from the inner loop and is able to handle many gradient steps without memory constraints. In addition [27], proposes methods to reduce the computation overhead of meta-training MAML for large tasks. Note that, in all these cases, savings arise from working around the limitations of MAML, while LITE is more general.

5 Experiments

In this section, we demonstrate that meta-learners trained with LITE achieve state-of-the-art performance among meta-learners on two challenging few-shot classification benchmarks: (i) ORBIT [14] which is a real-world few-shot object recognition dataset for teachable object recognizers; and (ii) VTAB+MD [11] which is composed of the Visual Task Adaptation Benchmark (VTAB) [20] and Meta-Dataset (MD) [13] and combines both few-shot and transfer learning tasks. We compare LITE meta-learners with state-of-the-art meta-learning and transfer learning methods in terms of classification accuracy, computational cost/time to learn a new task, and number of model parameters.

5.1 ORBIT Teachable Object Recognition Benchmark

Table 1: **Training meta-learners on large images with LITE achieves state-of-the-art accuracy with low test time adaption cost on ORBIT.** Results are reported as the average (95% confidence interval) over 85 test tasks (5 tasks per test user, 17 test users). I is image size. f is model trained with/without LITE. RN-18 is ResNet-18. EN-B0 is EfficientNet-B0. T is $\times 10^{12}$ MACs. F is forward pass. FB is forward-backward pass. Time is average wall clock time per task in seconds.

MODEL	I	f	Clean Videos		Clutter Videos		Test-time adaption			
			FRAME ACC	VIDEO ACC	FRAME ACC	VIDEO ACC	MACS	STEPS	TIME	PARAMS
			↑	↑	↑	↑	↓	↓	↓	↓
FineTuner [28]	84	RN-18	69.5 (2.2)	79.7 (2.6)	53.7 (1.8)	63.1 (2.4)	317.70T	50FB	53.94s	11.17M
	224	RN-18	72.2 (2.2)	81.9 (2.6)	56.7 (2.0)	61.3 (2.5)	546.57T	50FB	96.23s	11.18M
	224	EN-B0	78.1 (2.0)	85.9 (2.3)	63.1 (1.8)	66.9 (2.4)	121.02T	50FB	139.99s	4.01M
MAML [1]	84	RN-18	70.6 (2.1)	80.9 (2.6)	51.7 (1.9)	57.9 (2.5)	95.31T	15FB	36.98s	11.17M
	224	RN-18	75.7 (1.9)	86.1 (2.3)	59.3 (1.9)	64.3 (2.4)	163.97T	15FB	65.22s	11.18M
	224	EN-B0	79.3 (1.9)	87.5 (2.2)	64.6 (1.9)	69.4 (2.3)	36.31T	15FB	117.89s	4.01M
ProtoNets [3]	84	RN-18	65.2 (2.0)	81.9 (2.5)	50.3 (1.7)	59.9 (2.5)	3.18T	1F	0.73s	11.17M
	224	RN-18 + LITE	76.7 (1.9)	86.4 (2.2)	61.4 (1.8)	68.5 (2.4)	5.47T	1F	1.07s	11.18M
	224	EN-B0 + LITE	82.1 (1.7)	91.2 (1.9)	66.3 (1.8)	72.9 (2.3)	1.21T	1F	1.72s	4.01M
CNAPs [4]	84	RN-18	66.2 (2.1)	79.6 (2.6)	51.5 (1.8)	59.5 (2.5)	3.48T	1F	0.98s	12.75M
	224	RN-18 + LITE	76.0 (1.9)	84.9 (2.3)	58.2 (1.9)	62.5 (2.5)	7.64T	1F	2.11s	12.76M
	224	EN-B0 + LITE	79.6 (1.9)	87.6 (2.2)	63.3 (1.9)	69.2 (2.3)	3.38T	1F	2.85s	10.59M
Simple CNAPs [5]	84	RN-18	70.3 (2.1)	83.0 (2.5)	53.9 (1.8)	62.0 (2.5)	3.48T	1F	1.01s	11.97M
	224	RN-18 + LITE	76.5 (2.0)	86.4 (2.2)	57.5 (1.9)	64.6 (2.4)	7.64T	1F	2.14s	11.97M
	224	EN-B0 + LITE	82.7 (1.7)	91.8 (1.8)	65.6 (1.9)	71.9 (2.3)	3.39T	1F	2.92s	5.67M

ORBIT [14] is a highly realistic few-shot video dataset collected by people who are blind/low-vision. It presents an object recognition benchmark task which involves personalizing (i.e. adapting) a

recognizer to each individual user with just a few (support) videos they have recorded of their objects. To achieve this, the benchmark splits data collectors into disjoint train, validation, and test user sets along with their corresponding objects and videos. Models are then meta-trained on the train users, and meta-tested on how well they can learn a test user’s objects given just their videos (on a user-by-user basis). The benchmark has two evaluation modes: how well the meta-trained model can recognize a test user’s objects in *clean* videos where there is only that object present, and in *clutter* videos where that object appears within a realistic, multi-object scene.

Experiments We meta-train ProtoNets [3], CNAPs [4] and Simple CNAPs [5] with LITE on tasks composed of large (224×224) images. We also meta-train first-order MAML on large images as a baseline. Since first-order MAML can process task support sets in batches, we simply reduce the batch size and do not need to use LITE. We compare all of the above to meta-training on tasks of small (84×84) images (i.e. the original baselines [14]). We also include a transfer learning approach, FineTuner [28], which freezes a pre-trained feature extractor and fine-tunes just the linear classifier for 50 optimization steps. For each model, we consider a ResNet-18 (RN-18) and EfficientNet-B0 (EN-B0) feature extractor, both pre-trained on ImageNet [29]. We follow the task sampling protocols described in [14] (see Appendices B and C.1 for details). We also include analyses on meta-training with small tasks of large images in Appendix D.3.

Results In Table 1, we report frame accuracy and video accuracy, averaged over all the query videos from all tasks across all test users (17 test users, 85 tasks in total), along with their corresponding 95% confidence intervals. We also report the computational cost to learn a new task at test time in terms of the number of Multiply-Accumulate operations (MACs), the number of steps to adapt, and the wall clock time to adapt in seconds. See Appendix C.1 for results on additional metrics. The key observations from our results are:

- Training on larger (224×224) images leads to better performance compared to smaller (84×84) images. The boost is significant for both clean and clutter videos, though absolute performance remains lower on clutter videos. This suggests that object detection or other attention-based mechanisms may be required to further exploit large images in more complex/cluttered scenes.
- All meta-learners + LITE set a new state-of-the-art on clean videos, and perform competitively with the FineTuner on cluttered videos, using an EfficientNet-B0 backbone.
- Meta-learners are competitive with transfer learning approaches in accuracy but are almost two orders of magnitude more efficient in the number of MACs and the time to learn a new task, and one order of magnitude smaller in the number of steps to adapt.

5.2 VTAB+MD

VTAB+MD [11] combines revised versions of the Meta-Dataset (MD) and VTAB datasets and is one of the largest, most comprehensive, and most challenging benchmarks for few-shot learning systems. The MD-v2 part of the benchmark involves testing on 8 diverse datasets while VTAB-v2 involves testing on 18 datasets grouped into three different categories (natural, specialized, and structured).

Results Fig. 3 compares our best meta-learner, Simple CNAPs + LITE, with 6 other competitive approaches on VTAB+MD: BiT, MD-Transfer, and SUR are transfer learning based methods while ProtoMAML, ProtoNets, and CTX are meta-learning based. Note, comparisons are not always like-for-like as methods use differing backbones, image sizes, and pre-training datasets. Appendix D.2 provides this information along with the precise numbers and 95% confidence intervals. Appendices B and C.2 summarize all implementation and experimental details, and Appendix D.3 includes further analyses on the impact of task size on meta-training. The key observations from our results are:

- On MD-v2, Simple CNAPs + LITE has the highest average score and sets a new state-of-the-art.
- On VTAB-v2, BiT scores highest overall, but among meta-learners, Simple CNAPs + LITE is the best overall and on the natural and specialized sections. It falls short of CTX on the structured section due to poor performance on dSprites which involves predicting the position and orientation of small white shapes on a black background – a task quite different to image classification.
- These results are significant given that CTX takes 7 days to train on 8 GPUs, whereas Simple CNAPs + LITE trains in about 20 hours on a single 16GB GPU. In addition, Simple CNAPs + LITE uses a relatively small pre-trained backbone (4.0M parameters) compared to SUR’s 7 pre-trained ResNet-50s (one for each MD-v2 training set, plus ImageNet).

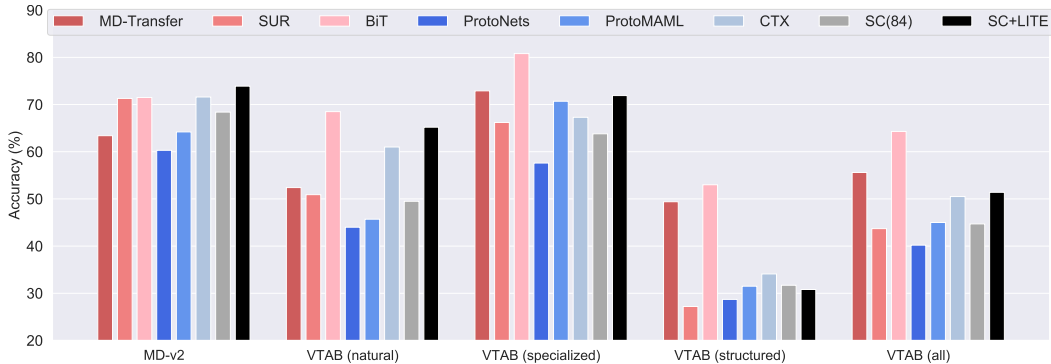


Figure 3: Summary of results on VTAB+MD. **Simple CNAPs with LITE (SC + LITE, black bar) trained on 224×224 images achieves state-of-the-art accuracy on Meta-Dataset (MD-v2), and state-of-the-art accuracy among meta-learners on 3 of 4 parts of VTAB.** As reference, we have included transfer learning methods (red bars), other meta-learning methods (blue bars), and Simple CNAPs without LITE trained on small images (84×84 , gray bar). Competitive results from [11]. See Table D.2 for tabular results on individual datasets.

- Simple CNAPs + LITE using 224×224 images significantly outperforms Simple CNAPs using 84×84 images, except for when the dataset images are small (e.g. Omniglot, QuickDraw, dSprites). This demonstrates that using large images and an approximation to the support set gradients achieves superior results compared to using small images with exact gradients.
- MD-Transfer and BiT perform strongly across VTAB+MD, however, Simple CNAPs + LITE is significantly faster to adapt to a new task requiring only a forward pass of the support set with no hyper-parameter tuning whatsoever. The transfer learners instead perform 100s of optimization steps to adapt to a new task and may require a human-in-the-loop to tune hyper-parameters such as the learning rate and number of optimization steps.

5.3 Effect of varying $|\mathcal{H}|$

Table 2 shows the effect of varying $|\mathcal{H}|$, the number of examples back-propagated per task, on the VTAB+MD benchmark. Performance is consistent across different $|\mathcal{H}|$, an expected result since LITE provides an unbiased estimate of the true gradient. For both Simple CNAPs and ProtoNets + LITE, the results at the lowest values of $|\mathcal{H}|$ are respectable, though they fall short of what can be achieved at $|\mathcal{H}| = 40$. Thus, the support gradient information does improve the solution, albeit by only 1-2 percentage points. Note, we report the lowest setting as $|\mathcal{H}| = 1$ for Simple CNAPs but $|\mathcal{H}| = 0$ for ProtoNets. This is because Simple CNAPs’s adaptation network (which processes the support set) shares no parameters with the feature extractor and thus will not be learned if the support gradients are completely ignored. On the other hand, ProtoNets’ adaptation network shares all its parameters with the feature extractor, thus can be meta-learned even when the support gradients are neglected.

Finally, in the two rightmost columns, we compare the classification accuracy for $|\mathcal{H}| = |\mathcal{D}_S|$ (i.e. using the full support set gradient) to $|\mathcal{H}| = 40$ (i.e. using LITE). Due to memory constraints, we do this at image size 84×84 . Here we see that the difference in accuracy is significant. We expect that performance will smoothly interpolate as $|\mathcal{H}|$ is increased from 40 to the size of the largest support set (at which point the full gradient is computed). This validates how LITE can be used to trade-off GPU memory usage for classification accuracy by varying $|\mathcal{H}|$. Furthermore, we conduct an empirical analysis (see Table D.7) which shows that the LITE gradient estimates and the gradients when using smaller sub-sampled tasks are unbiased w.r.t. the true gradients. However, Fig. 4 shows that LITE offers a significantly lower root mean square error w.r.t. the true gradients compared to using sub-sampled tasks at all but the highest values of $|\mathcal{H}|$. Refer to Appendix D.4 for additional details.

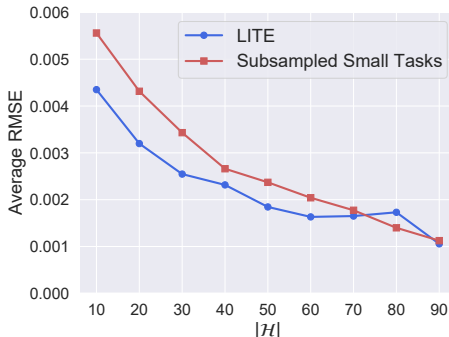


Figure 4: Average Root Mean Square Error (RMSE) w.r.t. the true gradients versus $|\mathcal{H}|$ for LITE and sub-sampled tasks on 84×84 images (10-way, 10-shot, $|\mathcal{D}_S| = 100$).

Table 2: Classification accuracy results in percent on VTAB+MD using Simple CNAPs and ProtoNets with varying values of $|\mathcal{H}|$. Image sizes are 224×224 and 84×84 pixels. For $|\mathcal{H}| > 40$, we used gradient/activation checkpointing methods [12] in addition to LITE. For full results see Appendix D.4

Model Image Size	Simple CNAPs 224×224						ProtoNets 224×224					Simple CNAPs 84×84	
$ \mathcal{H} $	1	10	20	30	40	100	0	10	20	30	40	40	$ \mathcal{D}_S $
MD-v2	72.8	73.7	73.3	73.8	73.9	74.3	71.0	72.0	72.0	72.5	72.7	63.6	68.4
VTAB (all)	51.2	51.0	50.5	51.1	51.4	51.2	45.1	45.8	46.2	46.2	46.1	42.7	44.7
VTAB (natural)	64.5	65.3	64.1	65.8	65.2	66.0	58.5	60.0	60.6	60.8	60.9	47.7	49.5
VTAB (specialized)	71.8	71.4	70.5	71.3	71.9	71.6	63.5	63.9	64.2	64.5	64.2	61.0	63.8
VTAB (structured)	31.0	30.0	30.3	29.9	30.8	29.9	26.0	26.2	26.4	26.1	25.9	29.9	31.7

6 Discussion

We propose LITE, a general and memory-efficient episodic training scheme for meta-learners that enables them to exploit large images for higher performance with limited compute resources. LITE’s significant memory savings come from performing a forward pass on a task’s full support set, but back-propagating only a random subset, which we show is an unbiased estimate of the full gradient. We demonstrate that meta-learners trained with LITE are state-of-the-art among meta-learners on two challenging benchmarks, ORBIT and VTAB+MD, and are competitive with transfer learning approaches at a fraction of the test time computational cost.

This offers a counterpoint to the recent narrative that transfer learning approaches are all you need for few-shot classification. Both classes of approach are worthy pursuits (and will need to exploit large images in real-world deployments) but careful consideration should be given to the data and compute available at test time to determine which class is best suited to the application under consideration. If it involves learning just a single task type (e.g. classifying natural images) with ample data and no compute or time constraints, then a fine-tuning approach would suffice and perform well. However, if a multitude of task types will be encountered at test time, each with minimal data, and new tasks need to be learned on resource-constrained devices (e.g. a mobile phone or a robot) or quickly/repeatedly (e.g. in continual or online learning settings), then a meta-learning solution will be better suited.

Finally, as the machine learning community grapples with greener solutions for training deep neural networks, LITE offers a step in the right direction by allowing meta-learners to exploit large images without an accompanying increase in compute. Future work may look toward applying the basic concept of LITE to other types of training algorithms to realize similar memory savings.

Limitations As discussed in Section 3, LITE can be applied to a wide range of meta-learners provided that they aggregate the contributions from a task’s support set via a permutation-invariant operation like a sum. Because only a subset of the support set is back-propagated, however, the gradients can be more noisy and meta-training may require lower learning rates. Furthermore, LITE is a memory-efficient scheme for training meta-learners episodically and has not been tried with meta-learners trained in other ways (e.g. with standard supervised learning) or non-image datasets.

Societal impact Few-shot learning systems hold much positive potential – from personalizing object recognizers for people who are blind [14] to rendering personalized avatars [30] (see [23] for a full review). These systems, however, also have the potential to be used in adverse ways – for example, in few-shot recognition in military/surveillance applications. Meta-trained few-shot systems may also pose risks in decision making applications as uncertainty calibration in meta-learning models has not yet been extensively explored. Careful consideration of the intended application, and further study of uncertainty quantification in meta-learning approaches will be essential in order to minimize any negative societal consequences of LITE if deployed in real-world applications.

Acknowledgments

We thank the anonymous reviewers for key suggestions and insightful questions that significantly improved the quality of the paper. Additional thanks go to Vincent Dumoulin for providing the tabular results for SUR used in Fig. 3 and Table D.2.

Funding Transparency Statement

Funding in direct support of this work: John Bronskill, Massimiliano Patacchiola and Richard E. Turner are supported by an EPSRC Prosperity Partnership EP/T005386/1 between the EPSRC, Microsoft Research and the University of Cambridge.

References

- [1] Chelsea Finn, Pieter Abbeel, and Sergey Levine. Model-agnostic meta-learning for fast adaptation of deep networks. In *Proceedings of the 34th International Conference on Machine Learning (ICML)*, pages 1126–1135, 2017.
- [2] Luisa M. Zintgraf, Kyriacos Shiarlis, Vitaly Kurin, Katja Hofmann, and Shimon Whiteson. Fast context adaptation via meta-learning. In *Proceedings of the 36th International Conference on Machine Learning (ICML)*, 2019.
- [3] Jake Snell, Kevin Swersky, and Richard Zemel. Prototypical networks for few-shot learning. In *Proceedings of the 31st Annual Conference on Neural Information Processing Systems (NeurIPS)*, pages 4077–4087, 2017.
- [4] James Requeima, Jonathan Gordon, John Bronskill, Sebastian Nowozin, and Richard E Turner. Fast and flexible multi-task classification using conditional neural adaptive processes. In *Proceedings of the 33rd Annual Conference on Neural Information Processing Systems (NeurIPS)*, pages 7957–7968, 2019.
- [5] Peyman Bateni, Raghav Goyal, Vaden Masrani, Frank Wood, and Leonid Sigal. Improved few-shot visual classification. In *Proceedings of the IEEE/CVF Conference on Computer Vision and Pattern Recognition (CVPR)*, pages 14493–14502, 2020.
- [6] Alexander Kolesnikov, Lucas Beyer, Xiaohua Zhai, Joan Puigcerver, Jessica Yung, Sylvain Gelly, and Neil Houlsby. Big transfer (bit): General visual representation learning. *arXiv preprint arXiv:1912.11370*, 6(2):8, 2019.
- [7] Mark B Ring. CHILD: A first step towards continual learning. *Machine Learning*, 28(1): 77–104, 1997.
- [8] David Saad. *On-line learning in neural networks*. Number 17. Cambridge University Press, 2009.
- [9] Steven CH Hoi, Doyen Sahoo, Jing Lu, and Peilin Zhao. Online learning: A comprehensive survey. *arXiv preprint arXiv:1802.02871*, 2018.
- [10] Antreas Antoniou, Massimiliano Patacchiola, Mateusz Ochal, and Amos Storkey. Defining benchmarks for continual few-shot learning. *arXiv preprint arXiv:2004.11967*, 2020.
- [11] Vincent Dumoulin, Neil Houlsby, Utku Evci, Xiaohua Zhai, Ross Goroshin, Sylvain Gelly, and Hugo Larochelle. Comparing transfer and meta learning approaches on a unified few-shot classification benchmark. *arXiv preprint arXiv:2104.02638*, 2021.
- [12] Tianqi Chen, Bing Xu, Chiyuan Zhang, and Carlos Guestrin. Training deep nets with sublinear memory cost. *arXiv preprint arXiv:1604.06174*, 2016.
- [13] Eleni Triantafillou, Tyler Zhu, Vincent Dumoulin, Pascal Lamblin, Utku Evci, Kelvin Xu, Ross Goroshin, Carles Gelada, Kevin Swersky, Pierre-Antoine Manzagol, and Hugo Larochelle. Meta-Dataset: A Dataset of Datasets for Learning to Learn from Few Examples. In *Proceedings of the 8th International Conference on Learning Representations (ICLR)*, 2020.
- [14] Daniela Massiceti, Luisa Zintgraf, John Bronskill, Lida Theodorou, Matthew Tobias Harris, Edward Cutrell, Cecily Morrison, Katja Hofmann, and Simone Stumpf. ORBIT: A Real-World Few-Shot Dataset for Teachable Object Recognition. In *Proceedings of the IEEE/CVF International Conference on Computer Vision (ICCV)*, 2021.

- [15] Oriol Vinyals, Charles Blundell, Timothy Lillicrap, Koray Kavukcuoglu, and Daan Wierstra. Matching networks for one shot learning. In *Proceedings of the 30th Annual Conference on Neural Information Processing Systems (NeurIPS)*, pages 3630–3638, 2016.
- [16] Sachin Ravi and Hugo Larochelle. Optimization as a model for few-shot learning. In *Proceedings of the 5th International Conference on Learning Representations (ICLR)*, 2017.
- [17] Jonathan Gordon, John Bronskill, Matthias Bauer, Sebastian Nowozin, and Richard Turner. Meta-learning probabilistic inference for prediction. In *Proceedings of the 7th International Conference on Learning Representations (ICLR)*, 2019.
- [18] Ethan Perez, Florian Strub, Harm De Vries, Vincent Dumoulin, and Aaron Courville. FiLM: Visual reasoning with a general conditioning layer. In *Proceedings of the 32nd AAAI Conference on Artificial Intelligence (AAAI)*, 2018.
- [19] Prasanta Chandra Mahalanobis. On the generalized distance in statistics. In *Proceedings of the National Institute of Science of India*, volume 12, pages 49–55, 1936.
- [20] Xiaohua Zhai, Joan Puigcerver, Alexander Kolesnikov, Pierre Ruysen, Carlos Riquelme, Mario Lucic, Josip Djolonga, Andre Susano Pinto, Maxim Neumann, Alexey Dosovitskiy, et al. A large-scale study of representation learning with the visual task adaptation benchmark. *arXiv preprint arXiv:1910.04867*, 2019.
- [21] Chen Sun, Abhinav Shrivastava, Saurabh Singh, and Abhinav Gupta. Revisiting unreasonable effectiveness of data in deep learning era. In *Proceedings of the IEEE/CVF International Conference on Computer Vision (ICCV)*, pages 843–852, 2017.
- [22] Nikita Dvornik, Cordelia Schmid, and Julien Mairal. Selecting relevant features from a multi-domain representation for few-shot classification. In *Proceedings of the European Conference on Computer Vision (ECCV)*, pages 769–786, 2020.
- [23] Timothy Hospedales, Antreas Antoniou, Paul Micaelli, and Amos Storkey. Meta-learning in neural networks: A survey. *arXiv preprint arXiv:2004.05439*, 2020.
- [24] Carl Doersch, Ankush Gupta, and Andrew Zisserman. CrossTransformers: spatially-aware few-shot transfer. *arXiv preprint arXiv:2007.11498*, 2020.
- [25] Alex Nichol, Joshua Achiam, and John Schulman. On first-order meta-learning algorithms. *arXiv preprint arXiv:1803.02999*, 2018.
- [26] Aravind Rajeswaran, Chelsea Finn, Sham Kakade, and Sergey Levine. Meta-learning with implicit gradients. In *Proceedings of the Annual Conference on Neural Information Processing Systems (NeurIPS)*, 2019.
- [27] Jaewoong Shin, Hae Beom Lee, Boqing Gong, and Sung Ju Hwang. Large-scale meta-learning with continual trajectory shifting. In *Proceedings of the International Conference on Machine Learning (ICML)*, 2021.
- [28] Jason Yosinski, Jeff Clune, Yoshua Bengio, and Hod Lipson. How transferable are features in deep neural networks? In *Proceedings of the 28th Annual Conference on Neural Information Processing Systems (NeurIPS)*, pages 3320–3328, 2014.
- [29] Jia Deng, Wei Dong, Richard Socher, Li-Jia Li, Kai Li, and Li Fei-Fei. ImageNet: A large-scale hierarchical image database. In *Proceedings of the IEEE/CVF Conference on Computer Vision and Pattern Recognition (CVPR)*, 2009.
- [30] Egor Zakharov, Aliaksandra Shysheya, Egor Burkov, and Victor Lempitsky. Few-shot adversarial learning of realistic neural talking head models. In *Proceedings of the IEEE/CVF International Conference on Computer Vision (ICCV)*, pages 9459–9468, 2019.
- [31] Kaiming He, Xiangyu Zhang, Shaoqing Ren, and Jian Sun. Deep residual learning for image recognition. In *Proceedings of the IEEE/CVF Conference on Computer Vision and Pattern Recognition (CVPR)*, pages 770–778, 2016.

- [32] Mingxing Tan and Quoc Le. EfficientNet: Rethinking model scaling for convolutional neural networks. In *Proceedings of the 36th International Conference on Machine Learning (ICML)*, pages 6105–6114, 2019.
- [33] Mark Sandler, Andrew Howard, Menglong Zhu, Andrey Zhmoginov, and Liang-Chieh Chen. Mobilenetv2: Inverted residuals and linear bottlenecks. In *Proceedings of the IEEE/CVF Conference on Computer Vision and Pattern Recognition (CVPR)*, pages 4510–4520, 2018.
- [34] Olga Russakovsky, Jia Deng, Hao Su, Jonathan Krause, Sanjeev Satheesh, Sean Ma, Zhiheng Huang, Andrej Karpathy, Aditya Khosla, Michael Bernstein, Alexander C. Berg, and Li Fei-Fei. ImageNet Large Scale Visual Recognition Challenge. *International Journal of Computer Vision (IJCV)*, 115(3):211–252, 2015. doi: 10.1007/s11263-015-0816-y.
- [35] Diederik Kingma and Jimmy Ba. Adam: A method for stochastic optimization. In *Proceedings of the 3rd International Conference on Learning Representations (ICLR)*, 2015.
- [36] TensorFlow Datasets, a collection of ready-to-use datasets. <https://www.tensorflow.org/datasets>, 2020.

A Applying LITE to meta-learners

A.1 CNAPs, Simple CNAPs + LITE

We show the LITE processing flow for both meta-training and meta-testing phases of CNAPs/Simple CNAPs in Fig. A.1. For each query set meta-training batch b , the support set images $\{x_{\mathcal{H}}, x_{\overline{\mathcal{H}}}\}$ are broken into batches, passed through a 2D conv net, then coalesced so that the pooling step can compute the mean of all the support set embeddings. This mean embedding is then passed into the FiLM parameter generator so that the feature extractor can be configured for the task. The support set images $\{x_{\mathcal{H}}, x_{\overline{\mathcal{H}}}\}$ are then passed through the adapted feature extractor in batches and the outputs are coalesced and then fed along with the support set labels $\{y_{\mathcal{H}}, y_{\overline{\mathcal{H}}}\}$ into the box labeled "Compute Classifier Params". For CNAPs, this box performs the class-conditional pooling operation and then uses an MLP to generate the weights and biases for the linear classifier. For Simple CNAPs, the same box computes the class-conditional means and covariances that are then used by the classifier in the Mahalanobis distance calculations. Once the classifier has been configured, the images in the query set batch $\{x_b^*\}$ can be classified and along with the true labels $\{y_b^*\}$, a loss is then computed. The meta-testing flow is similar, with the exception of the loss computation.

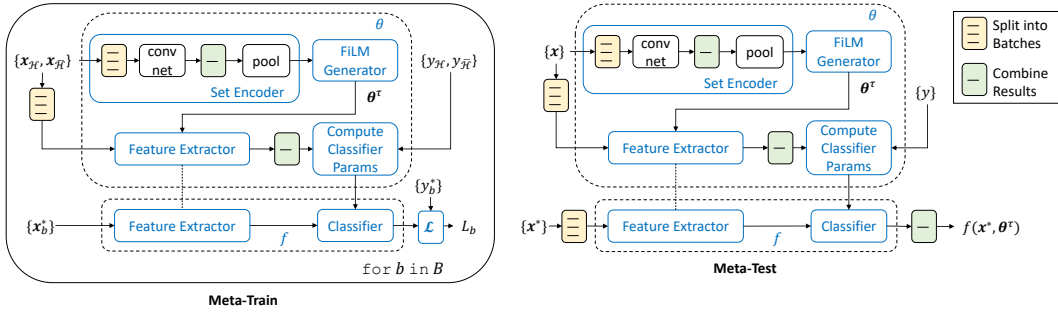


Figure A.1: CNAPs [4], Simple CNAPs [5] with LITE processing flow.

A.2 ProtoNets + LITE

We show the LITE processing flow for both meta-training and meta-testing phases of ProtoNets in Fig. A.2. For each query set meta-training batch b , the support set images $\{x_{\mathcal{H}}, x_{\overline{\mathcal{H}}}\}$ are broken into batches, passed through the feature extractor and the resulting embeddings are then combined. The combined embeddings along with the support set labels $\{y_{\mathcal{H}}, y_{\overline{\mathcal{H}}}\}$ are then used to compute the class prototypes. The query batch images $\{x_b^*\}$ are then passed through the feature extractor and the Euclidean distance from each query set image embedding to each of the class prototypes is computed. The predicted class is the one with the minimum distance. These predictions along with the true labels $\{y_b^*\}$ are used to compute the loss. The meta-testing flow is similar, with the exception of the loss computation.

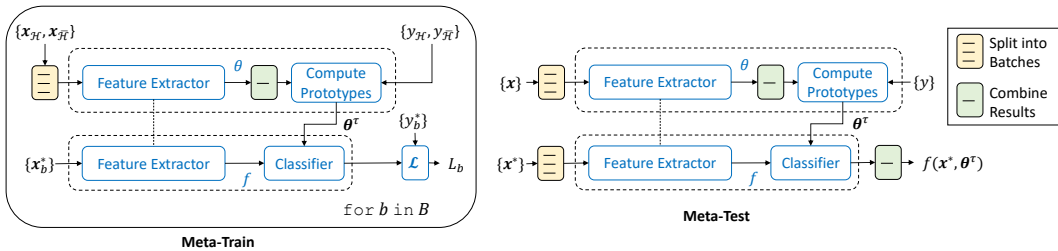


Figure A.2: ProtoNets [3] with LITE processing flow.

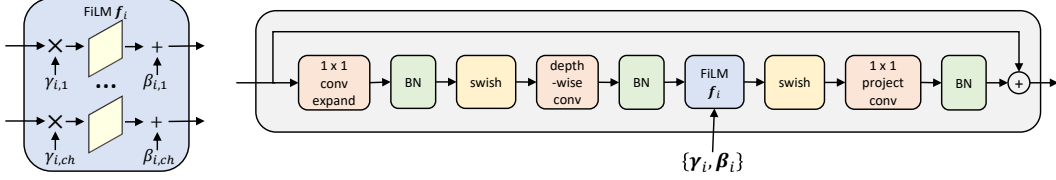


Figure B.3: (Left) A FiLM layer operating on convolutional feature maps indexed by channel ch . (Right) How a FiLM layer is used within a inverted residual block [33] of an EfficientNet [32].

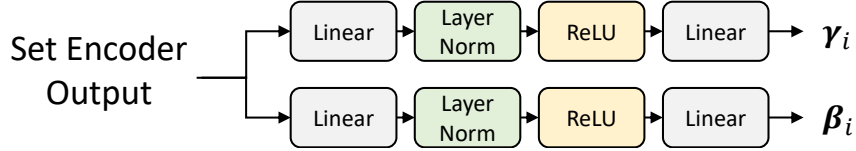


Figure B.4: Generator for i^{th} FiLM layer. The generator takes the output of the set encoder step for each task τ and passes it through the network to generate the parameters γ_i and β_i . The dimension of the vectors γ_i and β_i is equal to the number of feature channels at the location where the i^{th} FiLM layer is placed within feature extractor. The depicted generator network structure is repeated for each FiLM layer added to the feature extractor.

B Additional Simple CNAPs details

Our implementation of Simple CNAPs differs slightly from [5]. Here we describe the key architecture differences which were made with the goal of reducing the number of model parameters. We verified that these modification came without a reduction in classification performance:

- We replace the ResNet18 [31] feature extractor with an EfficientNet-B0 [32] since it has superior classification performance and fewer parameters (4.0M versus 11.2M for ResNet18). We pre-train the parameters of the feature extractor on ImageNet [29] and then freeze them during meta-training and meta-testing.
- Like Simple CNAPs, we use Feature-wise Linear Modulation (FiLM) layers [18] to adapt the feature extractor to the current task. In the EfficientNet-B0 feature extractor, we use a FiLM layer with scale parameters γ_i and offset parameters β_i after every separate convolutional layer and after every depth-wise separable convolution within a inverted residual block (refer to Fig. B.3). This is a total of 18 FiLM layers ($<0.2\%$ parameters in the model).
- We use a lower capacity 2-layer MLP network for generating parameters for each FiLM layer in the feature extractor (refer to Fig. B.4). This new FiLM layer generator network has less than 18% of the parameters (1.51M versus 8.45M) compared to the network used in the original Simple CNAPs.
- We do not use the Simple CNAPs Auto-regressive (AR) mode as the additional number of parameters did not yield sufficient gain.

Since the feature extractor parameters are frozen and the Mahalanobis distance based classifier has no parameters, the only learnable parameters in the model are in the set encoder and the network that generates the FiLM layer parameters.

C Experimental Details

In this section, we provide details for the LITE experiments using the ORBIT and VTAB+MD datasets.

C.1 ORBIT Teachable Object Recognition Benchmark

Meta-training and meta-testing for the ORBIT experiments were performed on a single NVIDIA Titan RTX with 24GB of memory.

Feature extractors We use either a ResNet-18 (following [14]) or an EfficientNet-B0 [32], both pre-trained on ImageNet [34]. Note, for CNAPs and Simple CNAPs, the feature extractor is frozen and only the set encoder and hyper-networks are trained, for ProtoNets and MAML all parameters are learned, and for the FineTuner the feature extractor is frozen and only the linear classifier is fine-tuned.

Meta-training protocol We train the learnable parameters in the meta-learners episodically on 50 randomly sampled tasks per train user per epoch (44 total train users). Note, each epoch samples 50 *new* tasks per train user. Each task is composed of clips sampled from a single user’s objects (random way) and associated videos (random shot). In the case of a large task, following [14], we randomly sample 4 clips from each support and query video, where each clip is 8 frames. For a small task, we limit this to 1 clip per support video and 1 clip per query video where each clip is 8 frames, and we also cap 1) the number of objects per task to 5, and 2) the number of support/query videos per object to 2. For both large and small tasks, a clip feature is taken as the average of its frame features, where each frame in 224×224 pixels. Note, the FineTuner undergoes no training – all feature extractor parameters are frozen to its pre-trained weights.

Meta-testing protocol Following [14], we evaluate the trained models on 5 tasks per test user, where each task is sampled from just that user’s objects and videos. Different to training, here each task contains *all* the test user’s objects and associated videos without caps. For each test task, we randomly sample 8 clips from each support video, and *all* overlapping clips from each query video. We then adapt the trained model to a task by using the task’s support clips to: i) perform a forward pass for CNAPs, Simple CNAPs and ProtoNets, ii) take 15 gradient steps on all the model’s parameters for MAML, or iii) take 50 gradient steps on just the linear classifier head for FineTuner. We evaluate the adapted model predictions for every clip in each query video in the test task (in the clean video evaluation mode, the query videos show just one object on a clear surface, while in the clutter video evaluation mode, the query videos show the object in a multi-object/cluttered scene). We report all metrics averaged over a flattened list of all the query videos from all tasks from all test users (17 test users, 85 tasks in total), along with its corresponding 95% confidence interval.

Optimization hyper-parameters For CNAPs, Simple CNAPs, and ProtoNets, we use the Adam optimizer [35] and a learning rate of 10^{-4} . For MAML, we use Adam and a learning rate of 10^{-5} for the outer loop, and Stochastic Gradient Descent (SGD) and a learning rate of 10^{-3} for the inner loop (rates reduced by 0.1 for the feature extractor in both loops). For the FineTuner, we use SGD and a learning rate of 0.1. We train Simple CNAPs with ResNet-18/EfficientNet-B0 for 10/15 epochs respectively, CNAPs for 15/15 epochs, ProtoNets for 20/20 epochs, and MAML for 20/20 epochs. These were chosen based on the number of learnable parameters in each model. Table 1 reports the test performance of the model with the best frame accuracy on a held-out validation set.

LITE hyper-parameters We train CNAPs, Simple CNAPs and ProtoNets with $H = 8$ clips (see Algorithm 1). We set the query batch size to $M_b = 8$ clips across all meta-learners. Note, MAML does not use LITE since we implement only the first-order variant. We, therefore, process support (and query) sets using standard batch processing with a batch size of 32 clips.

C.2 VTAB+MD Benchmark

Meta-training and meta-testing for the VTAB+MD experiments were performed on a single NVIDIA V100 16GB GPU. Meta-training takes about 20 hours.

Meta-training protocol Simple CNAPs + LITE uses an EfficientNet-B0 pretrained on ImageNet for the feature extractor f and all of its parameters are frozen and not updated during meta-training. As permitted in the VTAB+MD protocol, we meta-train Simple CNAPs + LITE in an episodic manner on the training splits of following datasets: ImageNet, Omniglot, Aircraft, CU Birds, DTD, QuickDraw, and Fungi. In addition, we meta-train on the test split of MNIST as it does not overlap with any of the test datasets. We meta-train for 10,000 iterations with the Adam [35] optimizer using a fixed learning rate of 0.001, and a batch size of 40. We back-propagate after every task, but do an optimization step after every 16 tasks.

Meta-testing protocol For meta-testing on MD-v2, we generate test episodes using the Meta-Dataset episode reader with the standard evaluation settings. We test all models with 600 episodes each on all test datasets. The classification accuracy is averaged over the episodes and a 95% confidence interval is computed. For each test dataset in VTAB-v2, we use the TensorFlow Datasets API [36] and randomly sample 1000 examples from the train split for the support set and use the entire test split for the query set and report a single accuracy.

D Additional Experimental Results

D.1 Full results on ORBIT benchmark

In the main paper, we report frame and video accuracy for test tasks, as well as the number of MACs and steps to adapt at test time and the number of model parameters. In Table D.1, we include a further metric – frames to recognition or FTR – which was proposed in the original baselines [14]. We also include additional results for large images (224) on small tasks without using LITE. Descriptions for the metrics are thus:

- **Frame accuracy**, the proportion of correct frame predictions in a query video;
- **Frames-to-recognition or FTR**, the number of frames before the first correct prediction, divided by the number of frames in the query video;
- **Video accuracy**, 1 if the most frequent frame prediction in a query video equals the true video label, otherwise 0;
- **MACs to adapt**, number of Multiply-Accumulate operations to learn a new task at test time (i.e. the operations required to process the whole support set);
- **Steps to adapt**, number of steps to learn a new task at test time (note, for gradient-based methods this involves multiple forward-backward passes through the model, while for amortization- and metric-based approaches this involves just a single forward pass);
- **Number of parameters**, number of learnable and frozen parameters in the model (note, this exclude the parameters that are generated by amortization-based methods)

Table D.1: Training meta-learners on large images with LITE achieves state-of-the-art accuracy with low test time adaption cost on the ORBIT Teachable Object Recognition Benchmark. Results are reported as the average (95% confidence interval) over 85 test tasks (5 tasks per test user, 17 test users). I is image size. f is model trained with/without LITE. RN-18 is ResNet-18. EN-B0 is EfficientNet-B0. T is $\times 10^{12}$ MACs. F is forward pass. FB is forward-backward pass. Time is average wall clock time per task in seconds.

MODEL	I f	Clean Videos			Clutter Videos			Test-time adaption			
		FRAME ACC ↑	FTR ↓	VIDEO ACC ↑	FRAME ACC ↑	FTR ↓	VIDEO ACC ↑	MACS ↓	STEPS ↓	TIME ↓	PARAMS ↓
FineTuner [28]	84 RN-18	69.5 (2.2)	7.8 (1.5)	79.7 (2.6)	53.7 (1.8)	14.4 (1.5)	63.1 (2.4)	317.70T	50FB	53.94s	11.17M
	224 RN-18	72.2 (2.2)	8.7 (1.7)	81.9 (2.6)	56.7 (2.0)	18.8 (1.8)	61.3 (2.5)	546.57T	50FB	96.23s	11.18M
	224 EN-B0	78.1 (2.0)	5.8 (1.4)	85.9 (2.3)	63.1 (1.8)	11.5 (1.4)	66.9 (2.4)	121.02T	50FB	139.99s	4.01M
MAML [1]	84 RN-18	70.6 (2.1)	8.6 (1.6)	80.9 (2.6)	51.7 (1.9)	21.0 (1.8)	57.9 (2.5)	95.31T	15FB	36.98s	11.17M
	224 RN-18	75.7 (1.9)	4.9 (1.2)	86.1 (2.3)	59.3 (1.9)	16.3 (1.7)	64.3 (2.4)	163.97T	15FB	65.22s	11.18M
	224 EN-B0	79.3 (1.9)	6.2 (1.4)	87.5 (2.2)	64.6 (1.9)	12.8 (1.5)	69.4 (2.3)	36.31T	15FB	117.89s	4.01M
ProtoNets [3]	84 RN-18	65.2 (2.0)	7.6 (1.4)	81.9 (2.5)	50.3 (1.7)	14.9 (1.5)	59.9 (2.5)	3.18T	1F	0.73s	11.17M
	224 RN-18	77.4 (1.8)	4.5 (1.1)	87.1 (2.2)	56.8 (1.8)	14.4 (1.5)	62.5 (2.5)	5.47T	1F	1.07s	11.18M
	224 RN-18 + LITE	76.7 (1.9)	5.1 (1.2)	86.4 (2.2)	61.4 (1.8)	13.2 (1.5)	68.5 (2.4)	5.47T	1F	1.07s	11.18M
	224 EN-B0	78.4 (1.8)	4.7 (1.1)	87.9 (2.1)	57.3 (1.8)	12.7 (1.4)	63.9 (2.4)	1.21T	1F	1.72s	4.01M
	224 EN-B0 + LITE	82.1 (1.7)	3.9 (1.0)	91.2 (1.9)	66.3 (1.8)	12.7 (1.5)	72.9 (2.3)	1.21T	1F	1.72s	4.01M
CNAPs [4]	84 RN-18	66.2 (2.1)	8.4 (1.4)	79.6 (2.6)	51.5 (1.8)	17.9 (1.7)	59.5 (2.5)	3.48T	1F	0.98s	12.75M
	224 RN-18	73.6 (2.0)	5.4 (1.2)	83.4 (2.4)	57.6 (1.8)	14.9 (1.6)	66.5 (2.4)	7.64T	1F	2.11s	12.76M
	224 RN-18 + LITE	76.0 (1.9)	5.9 (1.3)	84.9 (2.3)	58.2 (1.9)	15.1 (1.6)	62.5 (2.5)	7.64T	1F	2.11s	12.76M
	224 EN-B0	79.6 (1.9)	6.2 (1.4)	87.0 (2.2)	62.6 (1.9)	13.2 (1.5)	67.4 (2.4)	3.38T	1F	2.83s	10.59M
	224 EN-B0 + LITE	79.6 (1.9)	5.9 (1.3)	87.6 (2.2)	63.3 (1.9)	12.8 (1.5)	69.2 (2.3)	3.38T	1F	2.85s	10.59M
Simple CNAPs [5]	84 RN-18	70.3 (2.1)	7.3 (1.5)	83.0 (2.5)	53.9 (1.8)	16.0 (1.6)	62.0 (2.5)	3.48T	1F	1.01s	11.97M
	224 RN-18	75.2 (2.0)	6.0 (1.4)	84.6 (2.4)	58.1 (1.9)	14.7 (1.6)	60.9 (2.5)	7.64T	1F	2.13s	11.97M
	224 RN-18 + LITE	76.5 (2.0)	6.1 (1.4)	86.4 (2.2)	57.5 (1.9)	17.3 (1.7)	64.6 (2.4)	7.64T	1F	2.14s	11.97M
	224 EN-B0	81.4 (1.8)	4.9 (1.3)	88.3 (2.1)	65.6 (1.9)	11.2 (1.4)	69.9 (2.3)	3.39T	1F	2.91s	5.67M
	224 EN-B0 + LITE	82.7 (1.7)	4.1 (1.1)	91.8 (1.8)	65.6 (1.9)	13.5 (1.5)	71.9 (2.3)	3.39T	1F	2.92s	5.67M

D.2 Tabular results on VTAB+MD benchmark

In Table D.2, we show the tabular results for the VTAB+MD benchmark.

Table D.2: Classification accuracy results on VTAB+MD [11] using Simple CNAPs + LITE and various competing transfer learning and meta-learning approaches. All competitive results are from [11]. All figures are percentages and the \pm sign indicates the 95% confidence interval over tasks. Bold type indicates the highest scores (within the confidence interval). The VTAB-v2 results have no confidence interval as the testing protocol requires only a single run over the entire test set. RN indicates ResNet [31] and EN indicates EfficientNet [32]. The SUR results are with a linear classifier head. Simple CNAPs + LITE outperforms all approaches on MD-v2 and outperforms all meta-learning approaches on VTAB (all).

	Transfer learning				Meta-Learning			
	MD-Transfer	SUR	BiT	ProtoNets	ProtoMAML	CTX	SC(84)	SC+LITE
Backbone	RN-18	RN-50 x 7	RN-18	RN-18	RN-18	RN-34	EN-B0	EN-B0
Params (M)	11.2M	164.6M	11.2M	11.2M	11.2M	21.3M	4.0M	4.0M
Image Size	126	224	224	126	126	224	84	224
Omniglot	82.0 \pm 1.3	89.6	72.7 \pm 4.6	85.3 \pm 0.9	90.2 \pm 0.7	84.6 \pm 0.9	90.9 \pm 0.6	86.5 \pm 0.8
Aircraft	76.8 \pm 1.2	59.7	73.6 \pm 3.8	74.3 \pm 0.8	82.1 \pm 0.6	85.3 \pm 0.8	77.5 \pm 0.7	83.6 \pm 0.7
Birds	61.2 \pm 1.3	81.4	87.2 \pm 1.9	68.0 \pm 1.0	73.4 \pm 0.9	72.9 \pm 1.1	76.4 \pm 0.8	88.6 \pm 0.7
DTD	66.0 \pm 1.1	83.9	82.6 \pm 2.7	65.3 \pm 0.7	66.3 \pm 0.8	77.3 \pm 0.7	74.3 \pm 0.7	84.1 \pm 0.7
QuickDraw	61.3 \pm 1.1	81.2	66.3 \pm 3.6	60.6 \pm 1.0	66.4 \pm 1.0	73.3 \pm 0.8	76.5 \pm 0.7	75.7 \pm 0.8
Fungi	35.5 \pm 1.1	69.2	53.9 \pm 4.4	39.8 \pm 1.1	46.3 \pm 1.1	48.0 \pm 1.2	51.3 \pm 1.1	56.9 \pm 1.2
Traffic Sign	84.7 \pm 0.9	46.5	75.4 \pm 4.3	49.8 \pm 1.1	50.3 \pm 1.1	80.1 \pm 1.0	54.8 \pm 1.1	65.8 \pm 1.1
MSCOCO	39.6 \pm 1.0	58.6	60.0 \pm 2.9	39.7 \pm 1.0	39.0 \pm 1.0	51.4 \pm 1.0	45.1 \pm 1.0	50.0 \pm 1.0
Caltech101	70.6	86.5	84.6	72.0	73.1	84.2	79.6	87.7
CIFAR100	31.3	34.2	47.1	27.7	29.7	37.5	37.1	48.8
Flowers102	66.1	71.2	82.7	57.1	60.2	81.8	65.5	83.5
Pets	49.1	88.7	83.9	51.0	56.6	70.9	69.8	89.3
Sun397	13.9	0.5	29.1	14.2	8.1	24.8	18.0	30.9
SVHN	83.2	24.2	83.4	41.9	46.8	67.2	26.7	51.0
EuroSAT	88.7	82.6	93.8	77.7	80.1	86.4	82.8	89.3
Resisc45	63.7	67.8	74.1	50.8	53.5	67.7	64.5	76.4
Patch Camelyon	81.5	77.1	80.7	73.8	75.9	79.8	78.4	81.4
Retinopathy	57.6	37.4	74.5	28.0	73.2	35.5	29.4	40.3
CLEVR-count	40.3	34.1	55.2	32.0	32.7	27.9	30.7	31.4
CLEVR-dist	52.9	29.8	58.7	39.4	35.4	29.6	32.5	32.8
dSprites-loc	85.9	16.9	98.6	38.1	42.0	23.2	43.9	12.3
dSprites-ori	46.4	18.7	46.5	16.3	23.0	46.9	21.1	31.1
SmallNORB-azi	36.5	8.3	20.1	12.3	13.4	37.0	13.5	14.5
SmallNORB-elev	31.2	18.4	21.8	17.4	18.8	21.6	19.6	21.0
DMLab	43.0	33.5	43.7	31.8	32.5	31.9	33.9	39.4
KITTI-dist	58.7	57.5	78.8	42.1	54.4	54.3	58.1	63.9
MD-v2	63.4	71.3	71.5	60.3	64.2	71.6	68.4	73.9
VTAB (all)	55.6	43.7	64.3	40.2	45.0	50.5	44.7	51.4
VTAB (natural)	52.4	50.9	68.5	44.0	45.7	61.1	49.5	65.2
VTAB (specialized)	72.9	66.2	80.8	57.6	70.7	67.3	63.8	71.9
VTAB (structured)	49.4	27.2	53.0	28.7	31.5	34.1	31.7	30.8

D.3 Meta-training without LITE on small tasks with large images

Table D.3 we show classification results on VTAB+MD using various ablations of Simple CNAPs including LITE on versus off, image size 84×84 versus 256×256 pixels, and small versus large sized tasks. For the no LITE, image size 84×84 , and large task case, we meta-train on 35,000 tasks using the Adam optimizer at learning rate of 0.001 on the same training datasets as Simple CNAPs + LITE. For the no LITE, image size 224×224 pixels, and small task case, we meta-train on 15,000 tasks using the Adam optimizer at learning rate of 0.001 on the same training datasets as Simple CNAPs + LITE. To make the number of tasks small during meta-training, we limit the maximum support set size to be 40 and the maximum classification way to be 30.

It is clear that using larger images results in a significant boost in classification accuracy, except on datasets where the images are natively small (e.g. Omniglot, Quickdraw, dSprites). Using LITE versus a smaller task size results in a significant boost in classification accuracy on VTAB-v2 where the support set size is large (1000 examples), however the results on MD-v2, where the support set sizes are smaller, are very similar in the two cases.

The trend is similar in the case of the ORBIT dataset (refer to Table D.1) where the difference between using LITE and tasks with a smaller number of examples is not great (often within the margin of error). This is likely due to the fact that in the case of ORBIT (i) the classification way is typically

Table D.3: Classification accuracy results on VTAB+MD [11] using various ablations of Simple CNAPs including LITE on versus off, image size 84×84 versus 256×256 pixels, and small versus large tasks. All figures are percentages and the \pm sign indicates the 95% confidence interval over tasks. Bold type indicates the highest scores (within the confidence interval). The VTAB-v2 results have no confidence interval as the testing protocol requires only a single run over the entire test set. A pretrained EfficientNet-B0 [32] backbone was utilized in all runs. In general, using larger images leads to better results, and using LITE on large tasks greatly improves results on VTAB-v2.

LITE Task Size Image Size	No Large 84	No Small 224	Yes Large 224
Omniglot	90.9 \pm 0.6	91.6 \pm 0.6	86.5 \pm 0.8
Aircraft	77.5 \pm 0.7	81.5 \pm 0.7	83.6 \pm 0.7
Birds	76.4 \pm 0.8	88.8 \pm 0.6	88.6 \pm 0.7
DTD	74.3 \pm 0.7	83.7 \pm 0.6	84.1 \pm 0.7
QuickDraw	76.5 \pm 0.7	76.4 \pm 0.7	75.7 \pm 0.8
Fungi	51.3 \pm 1.1	59.3 \pm 1.1	56.9 \pm 1.2
Traffic Sign	54.8 \pm 1.1	60.7 \pm 1.0	65.8 \pm 1.1
MSCOCO	45.1 \pm 1.0	52.5 \pm 1.1	50.0 \pm 1.0
Caltech101	79.6	84.9	87.7
CIFAR100	37.1	50.2	48.8
Flowers102	65.5	78.9	83.5
Pets	69.8	87.7	89.3
Sun397	18.0	32.0	30.9
SVHN	26.7	37.6	51.0
EuroSAT	82.8	86.0	89.3
Resics45	64.5	69.8	76.4
Patch Camelyon	78.4	79.1	81.4
Retinopathy	29.4	40.2	40.3
CLEVR-count	30.7	28.7	31.4
CLEVR-dist	32.5	31.4	32.8
dSprites-loc	43.9	14.7	12.3
dSprites-ori	21.1	35.8	31.1
SmallNORB-azi	13.5	12.2	14.5
SmallNORB-elev	19.6	19.0	21.0
DMLab	33.9	36.7	39.4
KITTI-dist	58.1	57.0	63.9
MD-v2	68.4	74.3	73.9
VTAB (all)	44.7	49.0	51.4
VTAB (natural)	49.5	61.9	65.2
VTAB (specialized)	63.8	68.8	71.9
VTAB (structured)	31.7	29.4	30.8

small (less than or equal to 10); and (ii) since the support frames are derived from videos, there is significant redundancy in the support sets, making the difference between having a small and large number of support examples less important. The benefits of LITE are more apparent in tasks with large way and large support set sizes, as is the case with VTAB-v2.

D.4 Tabular results and additional details on the varying $|\mathcal{H}|$ experiments

Tables D.4 to D.6 provide full tabular results for classification accuracy versus varying $|\mathcal{H}|$ on VTAB+MD. Note that in Table D.6, using Simple CNAPS + LITE on images of size of 84×84 pixels with $|\mathcal{H}| = 40$, GPU memory usage drops to roughly 8 GB, which is approximately half of that used when run without LITE (i.e. $|\mathcal{H}| = |\mathcal{D}_S|$).

Table D.7 shows the mean squared error between the mean of the approximate gradients and the true gradients for both LITE and sub-sampled small tasks as $|\mathcal{H}|$ is varied. The low mean squared error values for both training methods empirically demonstrates that both are unbiased.

Table D.8 shows the average root mean squared error (RSME) of the approximate gradients and the true gradients for both LITE and sub-sampled small tasks as $|\mathcal{H}|$ is varied. Table D.8 and Fig. 4 show that the RMSE deviation of the LITE estimate is significantly smaller than that of sub-sampled small tasks at all but the highest values of $|\mathcal{H}|$. Note, that these results are limited to image classification in the specific networks and network parameters that we tested. Other data types and networks are left for future work.

These experiments were carried out as follows:

- The Simple CNAPS + LITE network is initialized identically for all runs.
- Image size is 84×84 pixels, so that the true gradients can be calculated.
- The same 10-way, 10-shot task ($|\mathcal{D}_S| = 100$) drawn from the DTD dataset is identical for all runs.
- Gradients are measured on the weights in the first (i.e. earliest) Conv2D layer in the set encoder after a single training iteration.
- Reference (exact) gradients are calculated without using LITE.
- Small task gradients are calculated by randomly sub-sampling the task (though we ensure there is at least one example per class).
- For each value of $|\mathcal{H}|$, the number of samples used in the calculations are chosen such that 1000 examples of the support set are used. For example, for $|\mathcal{H}| = 50$, 20 different one iteration training runs are done ($20 \text{ runs} \times 50 \text{ random examples per run} = 1000$).
- To calculate the values in Table D.7, for each value of $|\mathcal{H}|$, the mean of the approximate gradient runs is computed and then the mean squared error is computed between this value and the exact gradient.
- To calculate the values in Table D.8, for each value of $|\mathcal{H}|$, the RMSE between the approximate gradients and the exact gradients is computed and then this value is averaged over the number of runs.

D.5 Additional Results

Table D.9 contains the results for Simple CNAPS + LITE on VTAB+MD at image size 320×320 pixel with $|\mathcal{H}| = 10$, demonstrating that by employing LITE, even larger images can be used in meta-learning algorithms. Overall, these results are similar to the 224×224 case as the feature extractor was pre-trained at 224×224 pixels. However, on the Birds, Fungi, and Retinopathy datasets, where the original images are very large (> 320 pixels), the results on this run were better than the 224 case.

Table D.4: Classification accuracy results on VTAB+MD [11] using Simple CNAPs + LITE with varying values of $|\mathcal{H}|$. Image size is 224 x 224 pixels. To achieve $|\mathcal{H}| > 40$, we used gradient/activation checkpointing methods [12] in addition to LITE. All figures are percentages and the \pm sign indicates the 95% confidence interval over tasks. The VTAB-v2 results have no confidence interval as the testing protocol requires only a single run over the entire test set.

Dataset	$ \mathcal{H} = 1$	$ \mathcal{H} = 10$	$ \mathcal{H} = 20$	$ \mathcal{H} = 30$	$ \mathcal{H} = 40$	$ \mathcal{H} = 100$
Omniglot	83.5 \pm 1.0	85.2 \pm 0.9	85.5 \pm 0.9	85.9 \pm 0.9	86.5 \pm 0.8	86.2 \pm 0.8
Aircraft	82.1 \pm 0.8	82.9 \pm 0.8	82.5 \pm 0.8	83.5 \pm 0.7	83.6 \pm 0.7	83.4 \pm 0.8
Birds	88.0 \pm 0.7	89.4 \pm 0.5	88.9 \pm 0.6	88.5 \pm 0.7	88.6 \pm 0.7	88.8 \pm 0.7
DTD	84.4 \pm 0.7	84.3 \pm 0.7	84.2 \pm 0.7	85.1 \pm 0.6	84.1 \pm 0.7	85.1 \pm 0.7
QuickDraw	75.3 \pm 0.8	75.8 \pm 0.8	75.7 \pm 0.8	75.9 \pm 0.8	75.7 \pm 0.8	76.1 \pm 0.8
Fungi	53.8 \pm 1.2	55.3 \pm 1.2	56.8 \pm 1.2	56.5 \pm 1.2	56.9 \pm 1.2	57.2 \pm 1.2
Traffic Sign	65.9 \pm 1.1	66.6 \pm 1.1	64.7 \pm 1.1	64.7 \pm 1.1	65.8 \pm 1.1	65.9 \pm 1.1
MSCOCO	49.5 \pm 1.1	50.0 \pm 1.1	48.2 \pm 1.2	50.2 \pm 1.1	50.0 \pm 1.0	51.9 \pm 1.1
Caltech101	87.9	87.8	87.1	87.5	87.7	88.2
CIFAR100	46.8	46.6	45.2	48.1	48.8	50.1
Flowers102	82.8	83.8	82.9	83.7	83.5	83.0
Pets	89.2	89.2	89.3	89.5	89.3	89.7
Sun397	28.8	31.5	30.3	32.4	30.9	32.3
SVHN	51.4	53.0	49.6	53.5	51.0	52.7
EuroSAT	88.5	88.4	88.4	88.3	89.3	88.6
Resics45	75.3	75.1	74.4	75.9	76.4	76.1
Patch Camelyon	80.4	80.2	78.7	80.2	81.4	81.9
Retinopathy	42.8	42.0	40.4	40.7	40.3	39.8
CLEVR-count	31.0	29.0	30.4	29.7	31.4	30.9
CLEVR-dist	33.4	33.4	32.6	32.8	32.8	33.0
dSprites-loc	10.7	10.5	11.6	11.3	12.3	10.6
dSprites-ori	30.5	29.9	29.4	29.2	31.1	27.9
SmallNORB-azi	14.6	14	14.2	14.3	14.5	14.6
SmallNORB-elev	21.3	21.3	20.8	20.7	21	20.9
DMLab	40.4	40.6	40.3	38.5	39.4	38.8
KITTI-dist	65.7	61.5	63.3	63.0	63.9	62.4
MD-v2	72.8	73.7	73.3	73.8	73.9	74.3
VTAB (all)	51.2	51.0	50.5	51.1	51.4	51.2
VTAB (natural)	64.5	65.3	64.1	65.8	65.2	66.0
VTAB (specialized)	71.8	71.4	70.5	71.3	71.9	71.6
VTAB (structured)	31.0	30.0	30.3	29.9	30.8	29.9

Table D.5: Classification accuracy results on VTAB+MD [11] using ProtoNets with varying values of $|\mathcal{H}|$. Image size is 224 x 224 pixels. All figures are percentages and the \pm sign indicates the 95% confidence interval over tasks. The VTAB-v2 results have no confidence interval as the testing protocol requires only a single run over the entire test set.

Dataset	$ \mathcal{H} = 0$	$ \mathcal{H} = 10$	$ \mathcal{H} = 20$	$ \mathcal{H} = 30$	$ \mathcal{H} = 40$
Omniglot	86.7 ± 0.8	87.7 ± 0.8	88.3 ± 0.8	88.3 ± 0.7	88.3 ± 0.8
Aircraft	83.8 ± 0.7	84.6 ± 0.7	84.1 ± 0.7	85.1 ± 0.7	85.0 ± 0.7
Birds	88.8 ± 0.6	89.4 ± 0.6	89.8 ± 0.6	89.1 ± 0.7	90.2 ± 0.5
DTD	78.6 ± 0.6	79.7 ± 0.6	80.2 ± 0.7	80.6 ± 0.7	81.4 ± 0.6
QuickDraw	73.5 ± 0.8	75.0 ± 0.7	75.2 ± 0.8	75.6 ± 0.7	76.0 ± 0.7
Fungi	59.4 ± 1.2	58.9 ± 1.1	58.2 ± 1.2	58.0 ± 1.1	57.4 ± 1.1
Traffic Sign	50.0 ± 1.1	52.2 ± 1.1	52.1 ± 1.0	53.1 ± 1.1	53.5 ± 1.1
MSCOCO	47.3 ± 1.0	48.1 ± 1.0	48.1 ± 1.1	50.2 ± 1.0	49.8 ± 1.1
Caltech101	86.6	86.9	87.2	87.2	87.4
CIFAR100	35.5	39.6	42.0	43.4	43.1
Flowers102	76.6	77.9	78.3	78.5	78.2
Pets	88.5	88.4	88.7	88.7	88.6
Sun397	31.5	31.8	31.1	31.8	32.9
SVHN	32.0	35.6	36.4	35.3	35.2
EuroSAT	79.4	81.6	81.8	82.9	83.3
Resics45	65.7	67.4	68.0	69.0	68.8
Patch Camelyon	75.9	72.8	73.7	74.2	73.3
Retinopathy	32.9	33.7	33.2	31.9	31.3
CLEVR-count	28.3	27.3	27.1	27.2	27.2
CLEVR-dist	29.5	29.2	29.0	28.9	28.5
dSprites-loc	13.3	14.1	14.0	13.2	13.4
dSprites-ori	20.4	19.6	20.4	19.8	19.6
SmallNORB-azi	9.4	9.4	9.6	9.5	9.4
SmallNORB-elev	16.3	17.1	17.0	17.1	17.0
DMLab	35.2	35.5	35.9	35.9	35.8
KITTI-dist	55.6	57.2	58.2	57.1	56.5
MD-v2	71.0	72.0	72.0	72.5	72.7
VTAB (all)	45.1	45.8	46.2	46.2	46.1
VTAB (natural)	58.5	60.0	60.6	60.8	60.9
VTAB (specialized)	63.5	63.9	64.2	64.5	64.2
VTAB (structured)	26.0	26.2	26.4	26.1	25.9

Table D.6: Classification accuracy results on VTAB+MD [11] using Simple CNAPs + LITE with two values of $|\mathcal{H}|$. Image size is 84×84 pixels. All figures are percentages and the \pm sign indicates the 95% confidence interval over tasks. The VTAB-v2 results have no confidence interval as the testing protocol requires only a single run over the entire test set.

Dataset	$ \mathcal{H} = 40$	$ \mathcal{H} = D_S $
Omniglot	83.7 \pm 1.0	90.9 \pm 0.6
Aircraft	65.4 \pm 0.9	77.5 \pm 0.7
Birds	69.5 \pm 1.0	76.4 \pm 0.8
DTD	72.1 \pm 0.8	74.3 \pm 0.7
QuickDraw	70.6 \pm 0.9	76.5 \pm 0.7
Fungi	45.5 \pm 1.2	51.3 \pm 1.1
Traffic Sign	58.2 \pm 1.0	54.8 \pm 1.1
MSCOCO	43.8 \pm 1.1	45.1 \pm 1.0
Caltech101	74.9	79.6
CIFAR100	35.4	37.1
Flowers102	69.6	65.5
Pets	55.5	69.8
Sun397	13.9	18.0
SVHN	36.7	26.7
EuroSAT	84.2	82.8
Resics45	61.5	64.5
Patch Camelyon	74.0	78.4
Retinopathy	24.3	29.4
CLEVR-count	32.2	30.7
CLEVR-dist	36.3	32.5
dSprites-loc	26.5	43.9
dSprites-ori	19.7	21.1
SmallNORB-azi	14.0	13.5
SmallNORB-elev	19.0	19.6
DMLab	33.4	33.9
KITTI-dist	58.1	58.1
MD-v2	63.6	68.4
VTAB (all)	42.7	44.7
VTAB (natural)	47.7	49.5
VTAB (specialized)	61.0	63.8
VTAB (structured)	29.9	31.7

Table D.7: Mean Squared Error (lower is better) between the mean of the gradient estimates and the true gradients for both LITE and subsampled small tasks as $|\mathcal{H}|$ is varied. The task used was a 10-way, 10-shot task of 84×84 pixels from the DTD dataset. For each value of $|\mathcal{H}|$, 1000 support set examples were used.

Training Mode	10	20	30	40	$ \mathcal{H} $ 50	60	70	80	90
LITE	9.53E-11	9.24E-11	7.89E-11	8.48E-11	5.11E-11	5.31E-11	6.03E-11	1.02E-10	2.51E-11
Subsampled Small Task	9.23E-11	8.46E-11	7.67E-11	7.15E-11	6.45E-11	6.27E-11	5.67E-11	4.78E-11	4.30E-11

Table D.8: Average root mean squared error (lower is better) with respect to the exact gradients for both LITE and subsampled small tasks as $|\mathcal{H}|$ is varied. The task used was a 10-way, 10-shot task of 84×84 pixels from the DTD dataset. For each value of $|\mathcal{H}|$, 1000 support set examples were used.

Training Mode	10	20	30	40	$ \mathcal{H} $ 50	60	70	80	90
LITE	4.35E-03	3.20E-03	2.55E-03	2.32E-03	1.84E-03	1.63E-03	1.65E-03	1.73E-03	1.06E-03
Subsampled Small Task	5.56E-03	4.32E-03	3.43E-03	2.66E-03	2.37E-03	2.04E-03	1.77E-03	1.40E-03	1.13E-03

Table D.9: Classification accuracy results on VTAB+MD [11] using Simple CNAPs + LITE with $|\mathcal{H}| = 10$ and image size is 320×320 pixels. All figures are percentages and the \pm sign indicates the 95% confidence interval over tasks. The VTAB-v2 results have no confidence interval as the testing protocol requires only a single run over the entire test set.

Dataset	$ \mathcal{H} = 10, 320 \times 320$ pixels
Omniglot	83.2 \pm 1.0
Aircraft	82.5 \pm 0.8
Birds	91.2 \pm 0.6
DTD	85.3 \pm 0.7
QuickDraw	74.1 \pm 0.8
Fungi	58.0 \pm 1.2
Traffic Sign	62.4 \pm 1.1
MSCOCO	46.8 \pm 1.1
Caltech101	88.0
CIFAR100	45.2
Flowers102	82.6
Pets	89.5
Sun397	28.6
SVHN	51.9
EuroSAT	86.3
Resics45	72.7
Patch Camelyon	80.7
Retinopathy	46.4
CLEVR-count	30.8
CLEVR-dist	33.5
dSprites-loc	14.2
dSprites-ori	28.2
SmallNORB-azi	14.0
SmallNORB-elev	20.7
DMLab	40.3
KITTI-dist	62.3
MD-v2	72.9
VTAB (all)	50.9
VTAB (natural)	64.3
VTAB (specialized)	71.5
VTAB (structured)	30.5